Control Protocol Design and Analysis for Unmanned Aircraft System Traffic Management

Jiazhen Zhou, Dawei Sun, Inseok Hwang, *Member, IEEE*, and Dengfeng Sun, *Senior Member, IEEE*

***Abstract*— Due to the rapid development of technologies for small unmanned aircraft systems (sUAS's), the supply and demand market for sUAS's is expanding globally. With the great number of sUAS's ready to fly in civilian airspace, an sUAS aircraft traffic management system that can guarantee the safe and efficient operation of sUAS's is still absent. In this paper, we propose a control protocol design and analysis method for sUAS traffic management (UTM) which can safely manage a large number of sUAS's. The benefits of our approach are two-fold: at management level, the effort for monitoring sUAS traffic (authorities) and control/planning for each sUAS (operator/pilot) are both greatly reduced under our framework; and at operational level, the behavior of individual sUAS is guaranteed to follow the restrictions. Mathematical proofs and numerical simulations are presented to demonstrate the proposed method.**

***Index Terms*— Unmanned aircraft system traffic management, automatic control, artificial potential field.**

I. Introduction

WITH vast investments of financial support and research effort, sUAS's are envisioned to achieve autonomy based on the rapid development of their technologies including guidance, communication, sensing, and control. Commercial sUAS's have been developed for a variety of tasks, such as package delivery, rescue operations, photography, surveillance, infrastructure monitoring, etc. The market for sUAS's for civilian purposes is expanding rapidly among potential users including companies, governments, and hobbyists. With expectation of a great number of sUAS's operating in the airspace system, especially in urban environments, the control of sUAS behavior and management of their traffic are crucial for safety and efficiency [1]. With the above concerns, some rules and laws to regulate the operation of sUAS's in the civil domain have been published by the Federal Aviation Administration (FAA) [2]. However, a traffic management system that can ensure the enforcement of the rules and the efficiency of the system is absent.

The need for a sUAS Traffic Management (UTM) System has long been recognized with the increasing number of registered sUAS's. The FAA and NASA are leading efforts to make the rules and conduct the research on the large scale sUAS operations. A build-a-little-test-a-little strategy is currently used to address the UTM's scalability [3]. The UTM research is divided into four Technology Capability Levels (TCL) [4]:

- achieve rural sUAS operations for agriculture, firefighting and infrastructure monitoring.
- realize beyond-visual line-of-sight operations in sparsely populated areas, and provide flight procedures and traffic rules for longer-range applications.
- include cooperative and uncooperative sUAS tracking capabilities to ensure collective safety of manned and unmanned operations over moderately populated areas.
- involve sUAS operations in higher-density urban areas for tasks such as news gathering and package delivery, and large-scale contingency mitigation.

The flight tests for TCL 1 and TCL 2 have been successfully conducted in NASA's test sites, and basic requirements for sUAS operation in less populated areas have been proposed based on the test results [3], [5]. The discussions and tests on airspace design, corridors, geofencing, severe weather avoidance, separation management, spacing, and contingency management are the main focuses and most challenging parts in TCL 3 and TCL 4 research. However, no results on TCL 3 and TCL 4 have been reported, to the best of our knowledge. On the other hand, a few works have conceptually discussed the architecture of the UTM system and identified its basic elements [6]–[8]. These works envision UTM based on the existing Air Traffic Management (ATM) system for crewed aircraft. Nevertheless, such a design may not be feasible for large scale operation or dense traffic in the sense that it requires features like flight authorizations, flight plan review/approval, external data services (weather, intruder), which may suffer from the curse of dimensionality.

To improve the scalability of the UTM, we note some key characteristics differentiating the sUAS operation from the existing crewed aircraft operation. For crewed aircraft, the human pilot is capable of directly controlling the behavior of an aircraft. In contrast, the human operator for sUAS with the remote control has to rely on the system's autonomous control and/or decision supporting tools to cope with the large scale operation and complicated operational environment [9]. Although this autonomous nature brings more challenges to sUAS hardware/software requirements and risk evaluation, it brings an opportunity for the UTM to administrate the sUAS's from a control systems perspective. The fact that the

Manuscript received March 14, 2020; revised February 26, 2021; accepted April 27, 2021. Date of publication June 9, 2021; date of current version September 1, 2021. This work was supported by the NSF under Award 1955890. The Associate Editor for this article was K. G. Vamvoudakis. *(Corresponding author: Jiazhen Zhou.)*

The authors are with the School of Aeronautics and Astronautics, Purdue University, West Lafayette, IN 47907 USA (e-mail: zhou733@purdue.edu).

Digital Object Identifier 10.1109/TITS.2021.3083675

behavior of an sUAS is more governed by the autopilot instead of the human operator reveals that the UTM may regulate the collective sUAS traffic behavior by adopting certain control protocols: if the sUAS's can agree on predefined control protocols in certain airspace, then collective safety/efficiency assurance for sUAS traffic can be converted to a control protocol design problem. By directly regulating the sUAS traffic behavior at the control level, UTM can reduce the effort for trajectory planning and reviewing significantly.

With the aforementioned idea in mind, we propose a control protocol design and analysis method to improve the scalability for the UTM. In this framework, we envision that the UTM is responsible for publishing control protocols for sUAS's operating in each basic traffic element such that the desirable collective traffic behavior is assured without reviewing the high dimensional trajectories of all sUAS's explicitly. The basic element of sUAS traffic network considered here is called a single *link*, which is an abstraction of "road" or "lane", proposed by NASA [10]. The main ingredient of our framework is the artificial potential field (APF) approach for the control of the behaviors of sUAS's in each link, which is motivated by successes of the APF approach in various aerospace applications such as aircraft guidance law design [11], conflict resolution [12], and multi-agent control [13]. Upon the agreement of a set of APF functions in the control protocol, sUAS's can achieve the desired collective behaviors, such as collision avoidance, boundary clearance, and speed regularization. Our framework, at its core, converts the problem of sUAS traffic control to an APF-based decentralized control protocol design problem, which is similar to flocking control. A commonly accepted definition for flocking behavior is given by Reynolds rules [14]: 1) stay close to nearby flockmates, 2) avoid collision with nearby flockmates, and 3) attempt to match the velocity with nearby flockmates. For safe UTM operation, collision avoidance is crucial, and the velocity of each sUAS should conform to the desired/reference speed associated with the link. A representative design of APF-based flocking control has been introduced by Olfati-Saber [15]. Following this work, variants of distributed flocking algorithms have been proposed, i.e., the flocking algorithm under time varying communication network topology [16], the flocking algorithm that considers complex robotics models with non-holonomic constraints [17]–[21], and the hybrid flocking algorithm for fixed-wing aircraft [22]. Given the feedback nature of APF-based control design, the APF-based control law offers more robustness to model and environmental uncertainty in practice. For more rigorous treatment of robust APF-based control, we refer to [23], [24].

It should be noted that our problem of APF-based control protocol design and analysis for the UTM is different from any existing flocking control problems. For the flocking algorithm design, even though the collective system of interest has a multi-agent nature, the system consists of a fixed group of sUAS's. However, in our problem, the system of interest consists of sUAS's in a certain traffic link, which is time varying in the sense that some sUAS's may enter the link and some sUAS's may leave the link at some time instances. From the traffic management perspective, it is desired to investigate the sufficient conditions for the sUAS's to enter the traffic link without causing collision. The answer to such a problem is related to the analysis of the APF-based control protocol design using the Hamiltonian function (which is commonly used as an analogue to the concept of "energy" [15]). Since it is known that the collision avoidance can be guaranteed by limiting the "energy", a convergence rate of the "energy" can be used to estimate the upper bound of the "energy" at given a time instance, which estimates the incremental "energy" allowable to enter the traffic link at a given time to avoid collision. The incremental "energy" can be related to the entry rate or capacity of a traffic link. Indeed, the most challenging part of our theoretic analysis lies in establishing the convergence rate of the proposed control protocol, which has not been discussed in general flocking control problems.

The contributions of this work are: 1) We develop a control protocol design and analysis method which can safely manage sUAS traffic, while improving the scalability of the UTM. The problem of the collective behavior regularization and safety assurance is formally defined based on control theory; 2) After a formal definition of the sUAS traffic regularization, we design a distributed control protocol for sUAS in a single traffic link. Based on the convergence property of our control algorithm, we propose conditions on sUAS's for safely entering a traffic link; and 3) Based on our control protocol, we propose hardware/software requirements on sUAS's operating in the large scale traffic system.

The rest of the paper is organized as follows. Section II identifies the roles and responsibilities of each element in the sUAS traffic system in our framework. Section III formally introduces the formulation of the sUAS traffic regularization in a single traffic link and offers theoretical results. Section IV demonstrates the results via illustrative numerical simulations. Finally, Section V draws the conclusions.

II. Elements in the sUAS Traffic System

We consider a basic network structure of the future large scale sUAS traffic. A network is a fundamental structure of the ground traffic and the air traffic, and thus the usage of such structure in the sUAS traffic has been envisioned by NASA [4]. The traffic network is defined as a set of nodes and links, and each link connects two nodes with specified locations. Each link commits a specified altitude block and corridor width where sUAS's can be flown from one location to the other. For each link, the authority may specify the desired speed, top speed, desired separation, and minimum separation for collision avoidance. One way to ensure all requirements are satisfied is to review every filed flight plan and make sure every restriction is satisfied. The flight plan is often a time-position 4D trajectory, and a certain resolution of the trajectory is required to achieve safety assurance. Such high-dimension, high-resolution trajectory checking can be overburdening for the UTM, which should be responsible for managing large scale sUAS operations. Another way to efficiently manage the traffic is to assign sUAS's control protocols to each individual traffic link, by which the collective safety of sUAS's traffic within each link can be guaranteed and restrictions can be satisfied via theoretical analysis.

Our framework redefines the roles and responsibilities of four main roles in the future sUAS traffic system, which are sUAS operators, the infrastructure, sUAS's, and the UTM. We explain each component in the order of design process:

1) UTM design
   - Network Definition:A traffic network need to be first defined in the construction of the UTM system. The network must include elements such as nodes, links, and virtual boundaries of each link. Each traffic link has regulations/rules for sUAS's traveling in it, e.g., the speed limit, minimum separation between sUAS's, minimum distance to the virtual boundaries, and feasible landing areas. Those regulations may or may not be shared through all links. Separated networks will be necessary for sUAS's of different types. For example, fixed-wing sUAS's and multi-copters will need different networks due to their distinct flight dynamics, cruising speeds and take-off/landing processes. The construction of the networks needs to be done in collaboration with law makers, such as the FAA.
   - Control Protocol Design: A set of control protocols can be designed for each link once the rules are defined. In order to have control protocols that are feasible for all sUAS's traveling in the network, a basic physical dynamics of sUAS's will be assumed. One can assume that the sUAS's are equipped with low level autopilot system such that a multi-copter can be viewed as a single integrator model [25], and a fixed-wing sUAS follows a Dubins car model on the horizontal plane and a double integrator in the vertical direction [22]. It is desired that under a common control protocol, sUAS's can achieve collective safety assurance and operational efficiency. During the operation, the control protocols are broadcast for each link, and sUAS's follow the control protocols after entering the links. Based on the control protocols, the UTM can propose hardware/software requirements on the on-board measurement/estimation or communication for sUAS's.
   - Control Protocol Selection: Different sets of control protocols need to be designed for each link to take into account different factors, such as weather, human activities, emergencies, etc [2]. During the operations, the best suited control protocols are selected for links and broadcast.
2) Operator
   - Low Level Control Design: The operators design the low level controllers, such as from thrust/voltage to accelerations, in order to follow the high level control protocols broadcast by the UTM.
   - Equipment: Each sUAS should be equipped with necessary sensors and filters to estimate its states and relative information such as the distance to neighboring sUAS's or obstacles so that the high level control protocol from UTM can be properly implemented. The sUAS's will need to equip with ports that can receive supervisory command from the UTM broadcast.
   - Operation: An operator will need to specify the origin, destination, and the sequence of links an sUAS will travel during a task.
3) Infrastructure
   - Broadcast: It is envisioned that broadcasting will be a good practice to share the control protocols for its benefits in contingency management [26]. In the event of contingency, a suitable set of control protocols can be broadcast across the affected airspace timely, and thus sUAS's in the airspace can have a safe and immediate response to the unexpected event.
   - Monitor: Cameras, LIDAR, and/or radars can also be equipped in the infrastructure to monitor the sUAS traffic and send alerts in the event of intruder attack or malfunction.
4) sUAS
   - State Estimation: During a mission, an sUAS needs to take measurements and estimate the states of itself and relative information with respect to other sUAS's or obstacles.
   - Control Execution: An sUAS receives and executes the control protocol from broadcast.
   - Control Protocol Switching: When arriving at a junction, multiple control protocols will be available. An sUAS selects the one specified by the operator before the mission and complete the transition from one link to another.

The overall framework of our design is summarized in Figure 1. It can be seen that in our framework, the operators will only need to determine the sequence of transitions between links. the UTM will only need to monitor the real time traffic situations during the daily operations. Collision free, speed limits and other requirements are fulfilled by the design of control protocols. The shift of control design from operators to the UTM allows the UTM to have a high authority over the behaviors of the sUAS's traveling in the network, and thus safety and efficiency can be guaranteed by the collective behavior of sUAS's in each link resulting from the common control strategy.

Each element of the future sUAS traffic system discussed above can be extensively studied. In this article, we limit our attention to one of the most important and challenging elements: the control protocol design and analysis. We develop models and theoretical frameworks for analyzing the sUAS traffic behavior in a single link from a control systems perspective. Our results can be applied to more common and complicated traffic network elements such as merge links and split links [27]. We present our results in details in the following section.

III. Problem Formulation and Controller Design

In this section, we formulate the problem of sUAS traffic regularization and present details about how to design and

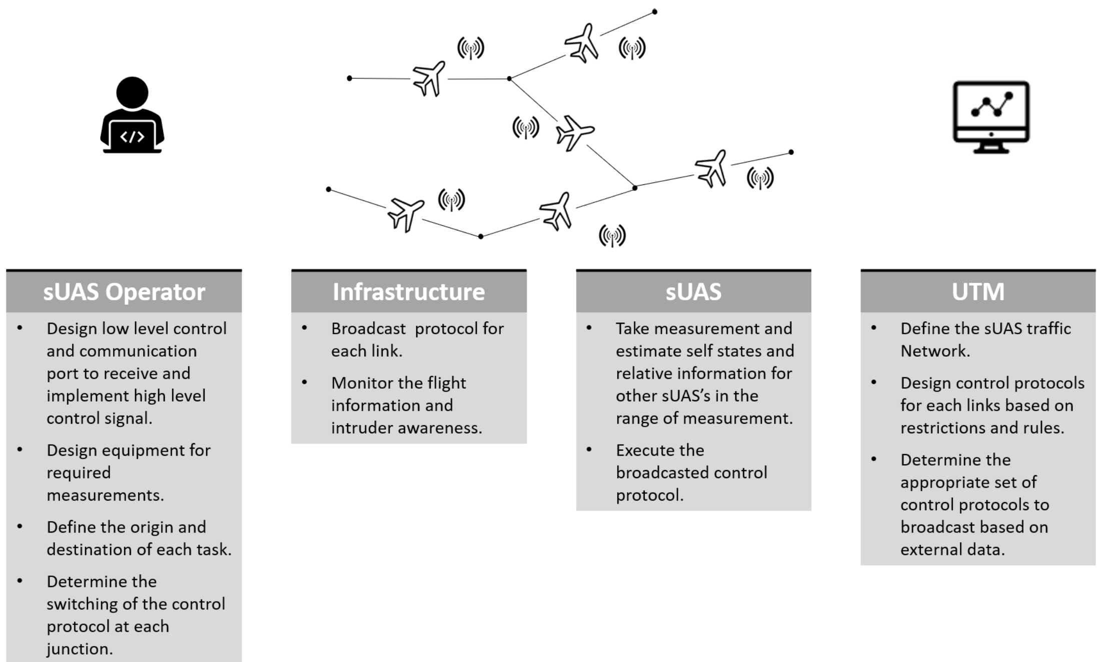

Fig. 1. Proposed UTM framework.

analyze control protocols to regulate the sUAS's behavior in a link using artificial potential functions. The objective of this section is to offer a guideline about how to design the APF for each link in an sUAS traffic network and what condition sUAS's should satisfy at entry of the link under a certain communication protocol structure such that the speed of all sUAS's in the link is regulated and there is no collision or boundary violations. The basic models for sUAS's and APF based control design are extensions from out previous work [22].

A. Dynamic Model for sUAS

In this section, we formally introduce the problem of regularization of sUAS traffic in a single link model. Let $\mathcal{I}$ be the index set of all the sUAS's in the traffic system. We consider a fixed-wing sUAS whose kinematics is described as:

$$\begin{aligned}\dot{x}_i &= \upsilon_i \cos\theta_i\\ \dot{y}_i &= \upsilon_i \sin\theta_i\\ \dot{z}_i &= w_i\\ \dot{\upsilon}_i &= a_i\\ \dot{\theta}_i &= \phi_i\\ \dot{w}_i &= \delta_i,\end{aligned} \tag{1}$$

where x_i and y_i are the horizontal coordinates, z_i is the vertical coordinate, θ_i is the horizontal heading angle, υ_i is the horizontal velocity, w_i is the vertical speed, and a_i, ϕ_i and δ_i are control inputs. By feedback linearizion, the horizontal dynamics can be converted to a double integrator model. Define $\upsilon_{xi} \triangleq \upsilon_i \cos\theta_i$, and $\upsilon_{yi} \triangleq \upsilon_i \sin\theta_i$. Then, we have:

$$\begin{bmatrix}\dot{\upsilon}_{xi}\\ \dot{\upsilon}_{yi}\end{bmatrix} = \begin{bmatrix}\cos\theta_i & -\upsilon_i \sin\theta_i\\ \sin\theta_i & \upsilon_i\cos\theta_i\end{bmatrix}\begin{bmatrix}a_i\\ \phi_i\end{bmatrix}. \tag{2}$$

Let $[u_{xi}, u_{yi}] = [\dot{\upsilon}_{xi}, \dot{\upsilon}_{yi}]$ be our new control input. We then have the following relation between the new and original control inputs:

$$\begin{bmatrix}a_i\\ \phi_i\end{bmatrix} = \begin{bmatrix}\cos\theta_i & \sin\theta_i\\ \dfrac{-\sin\theta_i}{\upsilon_i} & \dfrac{\cos\theta_i}{\upsilon_i}\end{bmatrix}\begin{bmatrix}u_{xi}\\ u_{yi}\end{bmatrix}. \tag{3}$$

The transformation is not defined for $\upsilon_i = 0$, which will not be the case for the fixed-wing sUAS. Now we have a double integrator dynamics for the fixed-wing sUAS:

$$\begin{aligned}\ddot{x}_i &= u_{xi}\\ \ddot{y}_i &= u_{yi}\\ \ddot{z}_i &= \delta_i.\end{aligned} \tag{4}$$

Finally we let $q_i \triangleq [x_i, y_i, z_i]^T$ be the state vector, $u_i \triangleq [u_{xi}, u_{yi}, \delta_i]$ be the control input vector. We call the stack vector $q \triangleq \mathrm{col}(q_1, q_2, \ldots)$ the configuration of the group sUAS's. The above model simplifies our process for designing control protocols. This also admits that our following approaches can be easily adopted in control protocol design for multi-copters whose dynamics can be approximated by a double integrator.

B. Problem Formulation

Here we introduce the problem formulation for traffic regulation for a single link. A single link is defined as a tuple $L \triangleq (\Omega, \hat{\upsilon}, \underline{\upsilon}, \overline{\upsilon}, \hat{d}, \underline{d}, \hat{d}_b, \underline{d}_b)$, where Ω is the physical space the link takes, $\hat{\upsilon}$ is the desired velocity for all sUAS's in Ω, $\underline{\upsilon}$, $\overline{\upsilon}$ are the top speed and lowest speed respectively, $\hat{d}$ is the desired separation between the sUAS's, and $\underline{d}$ is the minimum separation allowed between sUAS's. $\hat{d}_b$ is the desired distance to the boundaries of the link, and $\underline{d}_b$ is the minimum separation to the boundary of the link. Note that $\hat{v}$ is a velocity vector. We assume that Ω is a convex polyhedron, i,e., $\Omega = \{x|Ax \le b, \partial Ax \le \partial b\}$, where $A \in \mathbb{R}^{m\times 3}$ and $b \in \mathbb{R}^m$ representing m walls/boundaries; $\partial A \in \mathbb{R}^{m'\times 3}$ and $\partial b \in \mathbb{R}^{m'}$ denote m' entrances/exit. When the link is described by a rectangular tube, then $m = 4$, and $m' = 2$. Let A_n and b_n be the n_{th} row of A and b, respectively. Then, A_n is on the normal direction of the n_{th} wall. Denote the distance from the i_{th} sUAS's to the plane $A_n x = b_n$ as d_{in}. Then, d_{in} can be given as:

$$d_{in} = \frac{A_n q_i - b_n}{A_n A_n^T}. \tag{5}$$

We assume that the set

$$\mathcal{A} \triangleq \bigcap_{n=1}^{m}\{x|\frac{A_n x - b_n}{A_n A_n^T} \le \hat{d}_b\} \bigcap \{x|\partial Ax \le \partial b\} \tag{6}$$

is not empty. $\mathcal{A}$ represents the desired flying space within a link. It is clear that the reference velocity should be parallel to each plane, i.e., $\forall n,\ \hat{v}^T A_n = 0$. We define the set:

$$\mathcal{I}_\Omega(t) \triangleq \{i \in \mathcal{I}|\exists\tau \in [t_0, t], q_i(\tau) \in \Omega\} \tag{7}$$

as the set of all the sUAS's which entered the link up to time t. We assume that the link is sufficiently long, which implies that all sUAS's that have entered the link Ω before t_0 stay in Ω. This allows us to formulate our first problem: if there is no sUAS entering Ω after t_0, i.e., $\forall t > t_0$, $\mathcal{I}_\Omega(t) = \mathcal{I}_\Omega(t_0)$, we have the following objectives in the asymptotic sense:

$$O_1: \ \forall i \in \mathcal{I}_\Omega(t_0), \quad \dot{q}_i(t) \to \hat{v} \text{ as } t \to \infty,$$
$$O_2: \ \forall i,\ j \in \mathcal{I}_\Omega(t_0), \quad ||q_i(t) - q_j(t)|| \ge \hat{d} \text{ as } t \to \infty,$$
$$O_3: \ \forall i \in \mathcal{I}_\Omega(t_0), \quad \forall n = 1\ldots m,\ d_{in} \ge \hat{d}_b \text{ as } t \to \infty,$$

subject to the following constrains:

$$C_1: \ \forall i \in \mathcal{I}_\Omega(t_0), \quad ||\dot{q}_i(t) - \hat{v}|| \in [\underline{v}, \overline{v}]\ \forall t \ge t_0,$$
$$C_2: \ \forall i,\ j \in \mathcal{I}_\Omega(t_0), \quad ||q_i - q_j|| \ge \underline{d}\ \forall t \ge t_0,$$
$$C_3: \ \forall i \in \mathcal{I}_\Omega(t_0), \quad \forall n = 1\ldots m,\ d_{in} \ge \underline{d}_b\ \forall t \ge t_0.$$

O_1 requires the velocities of all the sUAS's in the link converge to the desired velocity. O_2 requires that the separations of all the sUAS's are greater than the desired separation given sufficiently long time. O_3 requires that the positions of all the sUAS's in the link converge to the desired separation from the boundary. C_1 requires the boundedness of the velocities of all the sUAS: the upper bound is given from traffic authority, and the lower bound is required for the flyable trajectory for a fixed-wing sUAS. C_2 requires that the separations between sUAS must be greater than or equal to the minimum separation to ensure collision free. C_3 requires that all the sUAS's in the link must stay away from the boundary greater than or equal to minimum distance.

Second, if there are sUAS's entering Ω at time t_1, let $\mathcal{I}_\Omega(t_1^-)$ denote the set of the sUAS's already in the link up to time t_1, i.e.,

$$\mathcal{I}_\Omega(t^-) \triangleq \{i \in \mathcal{I}|\exists\tau \in [t_0, t), q_i(\tau) \in \Omega\}. \tag{8}$$

Then we have $\mathcal{I}_\Omega(t_1^-) \subsetneq \mathcal{I}_\Omega(t_1)$, and $\mathcal{I}_\Omega(t_1) \setminus \mathcal{I}_\Omega(t_1^-)$ is the set of entering sUAS's. In this case, only C_1, C_2, and C_3 need to be guaranteed under some conditions on the entry states which will be discussed. It should be remarked that sUAS i might be in the link initially and leaves the link at $t^* > t_0$, but by our definition of $\mathcal{I}_\Omega(t)$, $i \in \mathcal{I}_\Omega(t)$ for any $t > t_0$. It is equivalent to assumption that the link is infinitely long such that whenever an sUAS enters it, it stays in it. This assumption facilitates the problem formulation and analysis without loss of generality, and it can be relaxed based on the approach in this work.

C. Control Protocol Design and Analysis

According to the control objectives and constraints, an APF-based control protocol is introduced in this subsection, which ensures O_1-O_3 and C_1-C_3 are satisfied assuming no sUAS enters the link Ω, i.e.,

$$\mathcal{I}_\Omega(t) = \mathcal{I}_\Omega(t_0), \quad \forall t > t_0. \tag{9}$$

The convergence rate of the control protocol will be discussed, based on which the entry condition that is established in the next subsection.

For a smooth artificial potential field design, the σ-norm function $||\cdot||_\sigma : \mathbb{R}^n \to \mathbb{R}_+$ is commonly considered [15]:

$$||z||_\sigma = \frac{1}{\varepsilon}(\sqrt{1 + \varepsilon||z||^2} - 1), \tag{10}$$

where $\varepsilon > 0$ is a parameter, and $||\cdot||$ is the Euclidean norm. σ-norm is an approximation for the Euclidean norm but equipped with the differentiability at $z = 0$. The gradient of σ-norm is given as:

$$\nabla||z||_\sigma = \frac{z}{\sqrt{1 + \varepsilon||z||^2}}. \tag{11}$$

For a nonzero vector d, denote $d_\sigma = ||d||_\sigma$, and it can be shown that $||d|| > d_\sigma$. We let the monotone decreasing function $\psi : \mathbb{R}^+ \to \mathbb{R}^+$ be the repulsive potential function for collision avoidance, and $\phi : \mathbb{R}^+ \to \mathbb{R}$ be the gradient of ψ. ψ and ϕ satisfy:

$$\begin{aligned} \psi(d) = 0 &\iff d \ge \hat{d} \\ \phi(d) = 0 &\iff d \ge \hat{d} \\ \psi(d) > 0 &\iff 0 \le d < \hat{d}. \end{aligned} \tag{12}$$

Let V_p be the accumulated collision potential energy:

$$V_p = \frac{1}{2}\sum_i \sum_{j\ne i} \psi(||q_{ij}||_\sigma), \tag{13}$$

where

$$q_{ij} = q_i - q_j, \tag{14}$$

then V_p achieves the global minimum of 0 at $\forall i, j, \in \mathcal{I}_\Omega(t_0)$ with $i \ne j$, $||q_{ij}||_\sigma \ge \hat{d}$, thus, $||q_{ij}|| > \hat{d}$. Similarly, we let ψ_b be the potential function for boundary clearance and ϕ_b be the gradient of ψ_b such that (12) is satisfied with $\hat{d}$ replaced by $\hat{d}_b$. Let V_b be the accumulated boundary potential energy:

$$V_b = \sum_i \sum_n \psi_b(d_{in}). \tag{15}$$

V_b achieves the global minimum of 0 when $\forall i \in \mathcal{I}_\Omega(t_0)$, $\forall k \in \{1, \ldots, m\}$, $d_{in} \geq \hat{d}_b$. We define the accumulated kinetic energy as:

$$V_k = \frac{1}{2}\sum_i (\dot{q}_i - \hat{\upsilon})^T(\dot{q}_i - \hat{\upsilon}). \tag{16}$$

It is clear that V_k achieves the global minimum of 0 if $\forall i \in \mathcal{I}_\Omega(t_0)$, $\dot{q}_i = \hat{\upsilon}$. Then, the feedback control protocol is designed as:

$$u_i = -\sum_{j\neq i}\phi(||q_{ij}||_\sigma)\hat{q}_{ij} - \sum_{n=1}^{m}\frac{\phi_b(d_{in})A_n^T}{A_n A_n^T} - K_i(\upsilon_i - \hat{\upsilon}), \tag{17}$$

where:

$$\hat{q}_{ij} = \frac{q_{ij}}{\sqrt{1+\varepsilon||q_{ij}||^2}}, \tag{18}$$

where K_i is a tuning parameter whose design needs to address the physical capability of the sUAS. The first two terms of (17) are *gradient-based terms* [15] which act like repulsive forces for inter-sUAS collision avoidance and boundary clearance. They are the derivatives of the potential functions V_p and V_b with respect to q_{ij} and q_i respectively. The last term is the velocity regulation term which acts like a damper.

We can define the positive semi-definite Hamiltonian function:

$$H = V_p + V_k + V_b. \tag{19}$$

Note that the value of the Hamiltonian function $H(t)$ can measure the distance between the configuration of sUAS's system at t and the desired configuration. The following theorem shows O_1, O_2 and O_3 are achieved given that constraints C_1, C_2 and C_3 are satisfied all the time under the case where the $H(t_0)$ is not too large, assuming no sUAS enter the link after t_0.

Theorem 1: Consider a fixed group of sUAS's (1) in the link Ω*, with the initial configuration in the sublevel set of the Hamiltonian* $\Omega_c = \{(q(t_0), \dot{q}(t_0))|H(t_0) \leq c\}$ *applied with the control protocol (17) for* $t \geq t_0$*. The following holds:*

(i) $\dot{H}(t) \leq 0$, $\forall t \geq t_0$.

(ii) Almost every solution of the multi-sUAS system (1) converges to the desired configuration, i.e., an equilibrium where $\forall i, j \in \mathcal{I}_\Omega(t_0)$ *with* $i \neq j$, $\dot{q}_i = \hat{\upsilon}$, $d_{in} \geq \hat{d}_b$, $||q_{ij}|| \geq \hat{d}$.

(iii) If $c \leq c_1^* \triangleq \psi(||\underline{d}||_\sigma)$*, no pair of sUAS's violate the minimum separation, i.e.,* $\forall i, j \in \mathcal{I}_\Omega(t_0)$, $i \neq j$, $t > t_0$, $||q_{ij}(t)|| \geq \underline{d}$.

(iv) If $c \leq c_2^* \triangleq \frac{1}{2}\tilde{\upsilon}^2$*, where* $\tilde{\upsilon} = \min\{\overline{\upsilon} - ||\hat{\upsilon}||, ||\hat{\upsilon}|| - \underline{\upsilon}\}$*, then there is no speed violation, i.e.,* $\forall i \in \mathcal{I}_\Omega(t_0)$, $t > t_0$, $||\dot{q}_i|| \in [\underline{\upsilon}, \overline{\upsilon}]$.

(v) If $c \leq c_3^* \triangleq \psi_b(\underline{d}_b)$*, then minimum wall clearance is guaranteed, i.e.,* $\forall i \in \mathcal{I}_\Omega(t_0)$, $t > t_0$, $d_{in} \geq \underline{d}_b$.

Proof: (i) Denote $\delta\upsilon_i \triangleq \dot{q}_i - \hat{\upsilon}$. We then have:

$$\dot{H}(q, \dot{q}) = \sum_i \delta\upsilon_i^T u_i + \frac{d}{dt}\Big[\frac{1}{2}\sum_{j\neq i}\psi(||q_{ij}||_\sigma) + \sum_{n=1}^{m}\psi_b(d_{in})\Big] \tag{20}$$

By definition, we have:

$$\frac{d}{dt}\psi(||q_{ij}||_\sigma) = \phi(||q_{ij}||_\sigma)\hat{q}_{ij}^T(\dot{q}_i - \dot{q}_j)$$
$$\frac{d}{dt}\psi_b(d_{in}) = \frac{\phi_b(d_{in})A_n^T\dot{q}_i}{A_n A_n^T}. \tag{21}$$

Substituting the control protocol (17) into (20) yields:

$$\dot{H} = \sum_i -K_i\delta\upsilon_i^T\delta\upsilon_i. \tag{22}$$

(ii) Statement (i) implies that $\dot{H} \leq 0$ given that H is positive semidefinite. From LaSalle's invariance principle [28], all the solutions converge to the largest invariant set contained in $\mathcal{I} = \{(q, \dot{q})|\dot{H} = 0\}$. Starting from almost every initial configuration, the positions of all sUAS's eventually satisfy the desired separation and their velocities match the reference velocity.

(iii) By contradiction, suppose there exists $t_1 > t_0$, sUAS's i^* and j^* collide, i.e., $||q_{i^*j^*}(t_1)||_\sigma \leq ||\underline{d}||_\sigma$, and then given the monotonicity of ψ and $||q_{i^*j^*}||_\sigma = ||q_{j^*i^*}||_\sigma$, we have:

$$H(t_1) \geq \psi(||q_{i^*j^*}||_\sigma) + \frac{1}{2}\sum_{i\neq i^*, j^*}\sum_{j\neq i, i^*, j^*}\psi(||q_{i^*j^*}||_\sigma)$$
$$\geq c_1^* > c. \tag{23}$$

By Statement (ii), $\forall t > t_0$, $\dot{H}(t) \leq 0$, therefore $H(t_1) \leq H(t_0) = c < c_1^*$. Hence, we have produced a contradiction. The proof for Statement (iv) and (v) follows the same argument as the proof for Statement (iii), therefore omitted. □

Remark 1: The proof for the convergence of the group behavior of sUAS's is rather standard [15]. The convergence of the sUAS's configuration to the desired configuration is given by the monotonicity of the Hamiltonian function and the fact that invariant set $\mathcal{I}$ *is contained in the set of desired configuration. To achieve the constraints satisfaction, we define* c_1, c_2, *and* c_3 *as the minimum possible values of Hamiltonian under the corresponding constraint violation. By limiting the Hamiltonian for the initial configuration under* c_1, c_2, *or* c_3, *we argue that the corresponding constraint would not be violated due to the monotonicity of both the Hamiltonian and the potential functions. By letting the level set for initial configuration as* $\{(q(t_0), \dot{q}(t_0)|H(t_0) \leq c^*\}$, *where* $c^* = \min\{c_1^*, c_2^*, c_3^*\}$, *one can achieve* O_1, O_2, O_3 *for almost every initial configuration while* C_1, C_2, C_3 *are satisfied.*

It can be seen that under the adoption of LaSalle's invariance principle, the asymptotic convergence is given but without a convergence rate. The convergence rate of the Hamiltonian can be crucial for designing the entry condition for a link or estimating the behaviors of sUAS in a link for any given time instance. Now we study the convergence property for a fixed group of multi-sUAS system (4) with the control protocol (17). We start with the augmented system dynamics:

$$\ddot{q} + K\dot{q} + \nabla\Psi(q) = 0, \tag{24}$$

where K is the collective damping ratio/time constant, Ψ is the positive semi-definite collective potential function, and $\nabla\Psi$ is the gradient of Ψ. In the scope of sUAS regulation,

$\Psi(q)$ is simply $V_p(q) + V_b(q)$. It can be seen from (17) that K is a diagonal matrix with positive diagonal entries. Without loss of generality, we assume the diagonal elements of K are the same, such that K can be reduced to scalar. We will refer K as a scalar in the proceeding without further notification. Such a system is often referred as a gradient Hamiltonian system. The asymptotic convergence of (24) of different types has been extensively discussed; however, the convergence rate is rarely given [29]–[33]. It is noted that system (24) can also be viewed as a second order differential equation method for solving the following optimization problem:

$$\underset{q}{\text{minipage}}\ \Psi(q). \tag{25}$$

The convergence rate is still rarely discussed under the continuous time optimization framework or flocking control framework. Motivated by the lack of convergence rate analysis, we develop the following convergence result for the general Hamiltonian systems. We start with following assumptions on the smoothness of the potential function:

Assumption 1: $\nabla\Psi$ is differentiable and Lipschitz with constant L.

Assumption 2: $L \geq \frac{K^2}{8}$.

Assumption 1 is a general smoothness condition. It is equivalent that $\nabla^2\Psi$ exists and $\nabla^2\Psi \leq LI$, where I is the identity matrix. Assumption 2 is not restrictive either. If a function satisfies Assumption 2 with constant L, then it must satisfy Assumption 2 with $L' \geq L$. Thus, there always exists L' such that Assumptions 1 and 2 are both satisfied.

We provide the following lemma that will be used to establish the convergence rate for (24) in proceding theorem:

Lemma 1: For system (24), if Assumptions 1 and 2 hold and $\Psi(q(0)), \nabla\Psi(q(0))$, and $\dot{q}(0)$ are finite, then:

$$\inf_{\tau\in(0,t)} p\nabla\Psi(q(\tau))^T\nabla\Psi(q(\tau)) + r\dot{q}(\tau)^T\dot{q}(\tau) \leq \frac{1}{t}\Big(\frac{1}{2}||\alpha\nabla\Psi(q(0)) + \dot{q}(0)||_2^2 + (\alpha K + 1)\Psi(q(0))\Big) \tag{26}$$

where $p = \frac{8KL-K^3}{8L^2}$, $r = \frac{K}{4}$, and $\alpha = \frac{K}{2L}$.

Proof: Given the dynamic system (24), let Lyapunov-like functions be:

$$\begin{aligned} V_1 &= \frac{1}{2}||\alpha\nabla\Psi(q) + \dot{q}||_2^2 \\ V_2 &= (\alpha K + 1)\Psi(q) \\ V_3 &= \int_0^t p\nabla\Psi(q)^T\nabla\Psi(q) + r\dot{q}^T\dot{q}dt. \\ V &= V_1 + V_2 + V_3. \end{aligned} \tag{27}$$

Given Assumption 2, p is non-negative. Thus, V_1, V_2, and V_3 are positive semi-definite. The time derivative of V_1 is:

$$\begin{aligned} \dot{V}_1 &= (\alpha\nabla\Psi(q) + \dot{q})^T(\alpha\nabla^2\Psi(q)\dot{q} - K\dot{q} - \nabla\Psi(q)) \\ &= -\dot{q}^T(KI - \alpha\nabla^2\Psi(q))\dot{q} - \alpha\nabla\Psi^T\nabla\Psi(q) \\ &\quad + \nabla\Psi(q)^T(\alpha^2\nabla^2\Psi(q) - \alpha KI - I)\dot{q}. \end{aligned} \tag{28}$$

The time derivative of V_2 and V_3 are respectively:

$$\begin{aligned} \dot{V}_2 &= (\alpha K + 1)\nabla\Psi(q)^T\dot{q} \\ \dot{V}_3 &= p\nabla\Psi(q)^T\nabla\Psi(q) + r\dot{q}^T\dot{q}. \end{aligned} \tag{29}$$

Adding the derivatives gives:

$$\begin{aligned} \dot{V} &= -\dot{q}^T((K-r)I - \alpha\nabla^2\Psi(q))\dot{q} \\ &\quad - (\alpha - p)\nabla\Psi(q)^T\nabla\Psi(q) + \alpha^2\nabla\Psi(q)^T\nabla^2\Psi(q)\dot{q} \end{aligned} \tag{30}$$

Given $\Psi(q)$ is L-smooth, we have $\nabla^2\Psi \leq LI$. Under Assumption 2, by letting $r = \frac{K}{4}$ and $\alpha = \frac{K}{2L}$, we have:

$$\begin{aligned} \dot{V} &\leq -\frac{K}{4}\dot{q}^T\dot{q} - (\alpha - p)\nabla\Psi(q)^T\nabla\Psi(q) \\ &\quad + \alpha^2\nabla\Psi(q)^T\nabla^2\Psi(q)\dot{q} \\ &= -\frac{K}{4}(\dot{q}^T\dot{q} - \frac{K}{L^2}\nabla\Psi(q)^T\nabla^2\Psi(q)\dot{q} \\ &\quad + (\frac{2}{L} - \frac{p}{K})\nabla\Psi(q)^T\nabla\Psi(q)). \end{aligned} \tag{31}$$

By letting $p = \frac{8KL-K^3}{8L^2}$, we have

$$(\frac{2}{L} - \frac{p}{K})I \geq (\frac{K}{2L^2})^2\nabla^2\Psi(q)^T\nabla^2\Psi(q). \tag{32}$$

Thus,

$$\dot{V} \leq -\frac{K}{4}||\dot{q} + \frac{K}{2L^2}\nabla^2\Psi(q)\nabla(q)||_2^2 \leq 0. \tag{33}$$

Therefore:

$$V_1(t) + V_2(t) + V_3(t) \leq V_1(0) + V_2(0) + V_3(0), \quad \forall t \geq 0. \tag{34}$$

By the positive semi-definiteness of V_1 and V_2, we have:

$$\int_0^t p\nabla\Psi(q)^T\nabla\Psi(q) + r\dot{q}^T\dot{q}dt \leq V_1(0) + V_2(0). \tag{35}$$

which implies (26). □

Remark 2: Note that the RHS of inequality 26 is the scaled magnitude of $\ddot{q}(t)$. The LHS of inequality 26 is some quantities depends on the initial configuration. Lemma 1 reveals that the infimum of the scaled magnitude of $\ddot{q}(t)$ converges to zero at speed of $1/t$.

Remark 3: The significance of Lemma 1 does not limit to UTM applications. It is the first attempt for establishing the convergence rate result for a general class of Hamiltonian systems, as well as for the continuous time algorithm for solving non-convex optimization problem. It is not surprising that $O(\frac{1}{t})$ convergence is achieved, since such speed is well established for the first order methods of solving non-convex optimization problem. This result can be applied to the analysis for the behavior of general classes of controlled system, such as flocking control, nonlinear control for dissipative systems, to name a few. It can offer more interpretations for the system behavior under different contexts while specific understanding or structure of the system is present.

Note that Lemma 1 is not directly useful in our problem because it only provides an upper bound for the velocities and gradient forces, not for the Hamiltonian function. The following theorem provides an insight for convergence rate of Hamiltonian function under a proper assumption:

Theorem 2: Consider system (24) with Assumptions 1 and 2. Suppose there are positive numbers $\underline{\alpha}$, $\overline{\alpha}$ for the trajectory $q(t)$ such that

$$\underline{\alpha}\Psi(q) \leq \nabla\Psi(q)^T\nabla\Psi(q) \leq \overline{\alpha}\Psi(q). \tag{36}$$

Then,

$$H(t) \le \frac{\lambda}{t - t_0} H(t_0), \tag{37}$$

where

$$\lambda = \max\left\{2, 1/\underline{\alpha} p\right\} \max\left\{(\bar{\alpha}/\alpha^2 + \alpha K + 1), 1\right\}.$$

Proof:

Recall the definition of the Hamiltonian function and using (36), we have

$$\begin{aligned} H(t) &= \frac{1}{2} K \dot{q}(t)^T \dot{q}(t)^T + \Psi(q(t)) \\ &\le 2\frac{K}{4} \dot{q}(t)^T \dot{q}(t)^T + \frac{1}{\underline{\alpha} p} p \nabla\Psi(q(t))^T \nabla\Psi(q(t)) \\ &\le \lambda_1 \left(\frac{K}{4} \dot{q}(t)^T \dot{q}(t)^T + p \nabla\Psi(q(t))^T \nabla\Psi(q(t)) \right), \end{aligned} \tag{38}$$

where $\lambda_1 = \max\left\{2, 1/\underline{\alpha} p\right\}$. Taking infimum of both sides and using the monotonicity of $H(t)$, we have

$$\begin{aligned} H(t) &= \inf_{\tau \in (t_0, t)} H(\tau) \\ &\le \inf_{\tau \in (t_0, t)} \lambda_1 \left(\frac{K}{4} \dot{q}(t)^T \dot{q}(t)^T + p \nabla\Psi(q(t))^T \nabla\Psi(q(t)) \right) \\ &\le \frac{\lambda_1}{t - t_0} \left(\frac{1}{2} ||\alpha \nabla\Psi(q(t_0)) + \dot{q}(t_0)||^2 + (\alpha K + 1)\Psi(q(t_0)) \right), \end{aligned} \tag{39}$$

where we use the inequality (26) in Lemma 1. In addition, with (36), we have

$$\begin{aligned} &\frac{1}{2} ||\alpha \nabla\Psi(q(t_0)) + \dot{q}(t_0)||^2 \\ &\le \frac{1}{2} ||\alpha \nabla\Psi(q(t_0)) + \dot{q}(t_0)||^2 + \frac{1}{2} ||\alpha \nabla\Psi(q(t_0)) - \dot{q}(t_0)||^2 \\ &\le \alpha^2 \nabla\Psi(q(t_0))^T \nabla\Psi(q(t_0)) + \dot{q}(t_0)^T \dot{q}(t_0). \end{aligned} \tag{40}$$

Thus, we have

$$\begin{aligned} &\left(\frac{1}{2} ||\alpha \nabla\Psi(q(t_0)) + \dot{q}(t_0)||^2 + (\alpha K + 1)\Psi(q(t_0)) \right) \\ &\quad \le (\bar{\alpha}/\alpha^2 + \alpha K + 1)\Psi(q(t_0)) + \dot{q}(t_0)^T \dot{q}(t_0) \\ &\quad \le \lambda_2 H(t_0), \end{aligned} \tag{41}$$

where $\lambda_2 = \max\left\{(\bar{\alpha}/\alpha^2 + \alpha K + 1), 1\right\}$. Combining (39) and (41), we have

$$H(t) \le \frac{\lambda_1 \lambda_2}{t - t_0} H(t_0), \tag{42}$$

which concludes the proof. □

Remark 4: It is clear that when the sUAS's system is at a desired configuration, condition (36) holds. For q near the desired configuration, condition (36) can also be achieved by choosing proper artificial potential functions (e.g., locally quadratic functions near the desired configuration). The existence of $\underline{\alpha}$ and $\overline{\alpha}$ allows us to establish a direct convergence bound on the total Hamiltonian of the system. The inequality (36) may not be necessary for the convergence rate to hold, as one can see in the simulation results. Such results allow us to offer theoretical completeness for the proceeding results on sUAS entry condition design.

D. Entry Condition Design

In the last subsection, we have designed a control protocol based on APF and we have shown that the configuration of a fixed group of sUAS's converges to an invariant set in which all sUAS's maintain the desired separation and track the desired velocity for almost every initial configuration. The convergence rate of the Hamiltonian is proved for a fixed group of sUAS's. The reason for deriving this rather stronger convergence property is to quantify the speed of regulating the behaviors of the sUAS's in a link. For almost every initial condition, we are able to bound the total energy/Hamiltonian in a link at a given time instance. It allows us to derive the time when the link is ready to accept more sUAS's and to estimate the total amount of energy the incoming sUAS's can bring into the link. By bounding the energy carried by the incoming sUAS's for each fixed time interval, we are able to bound the total number of incoming sUAS's under assumptions. In this way, our framework can not only account for the micro level regularization of the sUAS's behaviors, but also offer theoretical characterization to the macro level traffic property, in particular, the flow rate of each traffic link. Such characterization allows further evaluation of the efficiency of the whole traffic network.

Let

$$\{t | \mathcal{I}_\Omega(t^-) \subsetneq \mathcal{I}_\Omega(t)\} \tag{43}$$

be the set of time instances when sUAS's enter Ω. This set is called the set of time instances of *regular entry*. Denote the k-th entry instance as t_k. To limit the entry frequency for sUAS's and to keep the Hamiltonian below desired threshold $\bar{h}$ (a natural selection of $\bar{h}$ could be c^* for safe operation), we consider the following assumption:

Assumption 3: $\forall k \in \mathbb{Z}_{\ge 0}$, $t_{k+1} - t_k \ge T$.

According to Theorem 2, we have following proposition:

Proposition 1: Consider the sUAS's in a link with Assumption 3. Assume that the conditions in Theorem 2 hold. Suppose $H(t_0) \le \bar{h}$ and for each entry instance t_k, $H(t_k) - H(t_k^-) \le h_\epsilon \le \bar{h}$. If T given in the Assumption 3 satisfies

$$T \ge \frac{\lambda \bar{h}}{\bar{h} - h_\epsilon}, \tag{44}$$

then $H(t) \le \bar{h}$, $\forall t \ge t_0$.

Such a result is desirable in the sense that if the entry rate is bounded, the Hamiltonian function value is bounded such that collision and boundary violations are excluded. Note that our definition of entry event allows multiple sUAS's enter the link simultaneously and Proposition 1 still applies. However, the result will be conservative considering the cases where there may be multiple sUAS's enter the link intermittently in a short time period with relatively regulated configuration. To address such cases, we consider the following definition for the intermittent entry event of multiple sUA'sS in a short time period.

t_k is said to be a time instance for a *multiple entry* event if there are multiple sUAS's enter the link at t_k and before $t_k + t_\epsilon$, where t_ϵ is a design parameter that should be small. Denote $\mathcal{I}_{\partial\Omega}(t_k)$ as the index set for the sUAS's enter the link during $[t_k, t_k + t_\epsilon)$. Let $t_{k+1} - (t_k + t_\epsilon) \ge T$ and $T \gg t_\epsilon$. Since

t_ϵ is small, it is of interest to establish entry conditions on sUAS's in $\mathcal{I}_{\partial\Omega}(t_k)$ such that the overall sUAS traffic behavior satisfies the constraints during $[t_k+\epsilon, t_{k+1})$. It is done by the following proposition:

Proposition 2: Consider sUAS with dynamics (1) in the link Ω with conditions in Theorem 2 valid. Let t_k, $k \in \mathbb{Z}_{\geq 0}$ be the time instances of entry events (either regular entry or multiple entry) with Assumption 3 valid. For all $k \in \mathbb{Z}_{\geq 0}$, assume $\forall i \in \mathcal{I}_{\partial\Omega}(t_{k+1})$, $j \in \mathcal{I}_{\Omega}(t_{k+1}^-)$, $\psi(||q_{ij}(t_{k+1}+t_\epsilon)||_\sigma) = 0$. Let

$$\begin{aligned} \kappa &= \max_{i\in\mathcal{I}_{\partial\Omega}(t_{k+1}+t_\epsilon)} \frac{1}{2}||\delta v_i(t_{k+1}+t_\epsilon)||_2^2 + \sum_{n=1}^{m}\psi_b(d_{in}) \\ \gamma &= \max_{i\neq j\in\mathcal{I}_{\partial\Omega}(t_{k+1}+t_\epsilon)} \frac{1}{2}\psi(||q_{ij}(t_{k+1}+t_\epsilon))||_\sigma). \end{aligned} \tag{45}$$

If

$$M\kappa + M(M-1)\gamma \leq c^*(1-\frac{\lambda}{T}), \tag{46}$$

where M is the maximum possible number of UASs that can enter the link between $[t_k, t_{k+\epsilon}]$, and then $\forall t \in \cup_k[t_k + t_\epsilon, t_{k+1})$, C_1, C_2, C_3 are satisfied.

Proof: By the given conditions, we have:

$$\begin{aligned} H(t_{k+1}+t_\epsilon) = &\sum_{i\in\mathcal{I}_{\Omega}(t_{k+1}^-)} \frac{1}{2}\delta v_i^T\delta v_i + \sum_{n=1}^{m}\psi_b(d_{in}) \\ &+ \frac{1}{2}\sum_{j\in\mathcal{I}_{\Omega}(t_{k+1}^-), j\neq i}\psi(||q_{ij}||_\sigma) \\ &+ \sum_{i\in\mathcal{I}_{\partial\Omega}(t_{k+1}+t_\epsilon)} \frac{1}{2}\delta v_i^T\delta v_i + \sum_{n=1}^{m}\psi_b(d_{in}) \\ &+ \sum_{i\in\mathcal{I}_{\Omega}^{\partial}(t_{k+1}+t_\epsilon), j\neq i}\psi(||q_{ij}||_\sigma) \end{aligned} \tag{47}$$

for any $k \in \mathbb{Z}_{\geq 0}$. Given that $H(t_k) \leq c^*$, and by Theorem 2, we have:

$$H(t_{k+1}^-) \leq \frac{c^*\lambda}{T}. \tag{48}$$

Thus,

$$\begin{aligned} H(t_{k+1}+t_\epsilon) \leq &\sum_{i\in\mathcal{I}_{\partial\Omega}(t_{k+1}+t_\epsilon)} \frac{1}{2}\delta v_i^T\delta v_i + \sum_{n=1}^{m}\psi_b(d_{in}) \\ &+ \frac{1}{2}\sum_{j\in\mathcal{I}_{\partial\Omega}(t_{k+1}+t_\epsilon), j\neq i}\psi(||q_{ij}||_\sigma) \\ &+ \frac{c^*\lambda}{T} \\ \leq &\, M\kappa + M(M-1)\gamma + \frac{c^*\lambda}{T}. \end{aligned} \tag{49}$$

Given $M\kappa + M(M-1)\gamma \leq c^*(1-\frac{\lambda}{T})$, we conclude that $H(t_{k+1}+t_\epsilon) \leq c^*$. By Theorem 1, C_1, C_2, and C_3 are satisfied $\forall t \in \cup_k[t_k+t_\epsilon, t_{k+1})$. □

Remark 5: The above proposition assumes that the distance between any sUAS entering the link at t_{k+1} and any sUAS already in the link before t_{k+1} is greater than or equal to the desired separation. Such assumption can be realized by the design of T for any given $\hat{v}$. It is also assumed that the boundedness of the Hamiltonian is satisfied all the time before the entry of the group of sUAS's. This assumption shall not be violated in practice to ensure safety.

We have established results for control-based single link traffic management. We showed that a fixed group of sUAS's configuration is regularized under our control law (Theorem 1). We also established the convergence rate of the Hamiltonian of the sUAS system (Theorem 2). With the convergence rate, we are able to estimate the allowable entry condition for constraints satisfaction (Proposition 2). In any traffic system, a traffic link is usually connected with one or multiple links. The entry traffic of one link is the exit traffic of the upstream link. We hereby assume that the exit traffic is at desired configuration of the upstream link and briefly discuss how Proposition 2 serves as a practical tool for link transition design. It is intuitive that two very "different" links should not be connected. The following discussion quantifies the maximum difference between two links in order to be connected. Let the upstream link and downstream link be $L_1 = (\Omega_1, \hat{v}_1, \underline{v}_1, \overline{v}_1, \hat{d}_1, \underline{d}_1, \hat{d}_{1b}, \underline{d}_{1b})$ and $L_2 = (\Omega_2, \hat{v}_2, \underline{v}_2, \overline{v}_2, \hat{d}_2, \underline{d}_2, \hat{d}_{2b}, \underline{d}_{2b})$, respectively. Let ψ^1, ψ_b^1 and ψ^2, ψ_b^2 be the potential energy functions used for the collision avoidance and the boundary clearance for L_1 and L_2, respectively. Assume that L_1 is long enough such that the exiting sUAS's are at desired configuration of L_1. We also define the event of link transition. sUAS i is said to transit from L_1 to L_2 if:

$$q_i \in \mathcal{A}_1 \cap \mathcal{A}_2. \tag{50}$$

This admits that $\mathcal{A}_1 \cap \mathcal{A}_2 \neq \emptyset$, and $\psi_b^1(d_{in}) = \psi_b^2(d_{in}) = 0$ for $n = 1, \ldots, m$. After a transition, sUAS's will start using the control protocol defined on L_2. Then κ and γ in (45) can be quantified based on the definitions of L_1 and L_2, that is:

$$\begin{aligned} \kappa &= \frac{1}{2}(\hat{v}_1 - \hat{v}_2)^T(\hat{v}_1 - \hat{v}_2) \\ \gamma &= \frac{1}{2}\psi^2(\hat{d}_1) \end{aligned} \tag{51}$$

It can be observed from (46) that if $\kappa \geq (1-\lambda/T)c^*$, then no more than one sUAS can enter L_2 from L_1 to ensure constrains satisfaction. This phenomenon explains that a high speed link should not be connected to a low speed link immediately, but another transitional link will be necessary. The idea of the transitional link resembles the on/off ramp of the highway in ground traffic. The maximum number of sUAS's that can enter L_2 from L_1 in every $[t_k, t_k+t_\epsilon)$ is then the maximum integer solution to inequality (46). This identity connects our analysis on the entry condition to the macro flow control between two connected links. It should be noted that our discussion on link transition only applies when the entering sUAS's are at desired configuration of the upstream link. For more complicated cases where the upstream link is too short for the sUAS's to achieve the desired configuration before exiting, it is of our interest to propose new system design or mathematical formulation to accommodate such a scenario in future research.

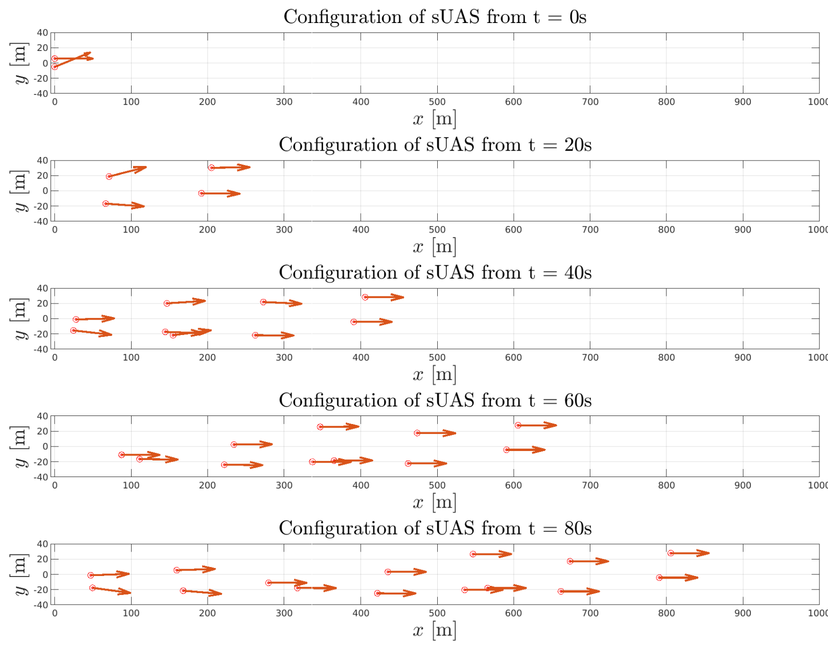

Fig. 2. Configurations of sUAS in every 20s after the entry of a new group of sUAS's.

E. Hardware/Software Requirement

In this section, we briefly discuss the hardware and software requirements on sUAS's for the implementation of the control protocols we designed. First, under our current framework, a receiver is required on an sUAS to receive the broadcast control protocol in each traffic link. Certain encoding and decoding protocols need to be designed in this process to prevent any potential cyberattack. The control protocol (17) first assumes that the position and velocity are estimated. This can be achieved by the integration of inertia measurement sensors, such as gyroscope, accelerometer, along with a Global Positioning System, which are typical equipped on an sUAS. Sensor fusion and state estimation techniques can be applied to achieve accurate state information for each sUAS. The subject of state estimation for highly non-linear sUAS dynamics is non trivial, and we refer to [34], [35] for more details. Second, for the inter-sUAS separation, the relative distance measurement is required. Unlike classic formation control or flocking control problems where a cooperative information exchange protocol is assumed, it may not be practical to assume that all sUAS's traveling in a traffic network can communicate the state information directly in a communication network. Therefore, the relative position measurement/estimation is required for our control protocol to be implemented. The existence of other sUAS's and obstacles are not differentiated, and obstacle sensing techniques can be used to achieve collision avoidance and desired separation. Detection sensors like radar, LIDAR, or sonar can be used to measure relative distances of approaching objects. It should be noted that in our control law, the relative positions for all other sUAS's are taken. This is not necessary in practice. Since the repulsive energy function ψ and repulsive force function ϕ have finite support, which means that an sUAS needs to take only relative position measurements for sUAS's/object in the range of $\hat{d}$. This can greatly reduce the requirements for measurements and computation for real-time sUAS control. Third, for the boundary clearance, it should be noted that the boundaries of traffic links are defined abstractly, taking factors such as human activities, regional weathers, emergencies, etc. The boundaries can vary in the day to day operations, and the distances to the boundaries are not to be directly measured by sensors. Instead, the boundaries data is stored in the A, b matrices, and the distances to the boundaries are evaluated by (5). Therefore, only self-position estimation is required in each sUAS to achieve boundary clearance. The A, b matrices are rather low-dimensional, and can be stored onboard before operation or broadcast by traffic management system. Combinations of sensors and data fusion techniques can be used to get more accurate state estimations. A comprehensive survey on sUAS sensing technologies can be found in [36].

TABLE I
PARAMETERS FOR SIMULATION

$\hat{v}$	$[10, 0, 0]^T$ [m/s]
$\overline{v}$	25 [m/s]
$\underline{v}$	5 [m/s]
$\underline{d}$	1.5 [m]
$\hat{d}$	10 [m]
$\underline{d}_b$	0 [m]
$\hat{d}_b$	20 [m]
K_i	0.1
ε	0.9
T	20 [s]

IV. NUMERICAL EXPERIMENTS

In this section, we demonstrate the proposed control protocol for UTM with an illustrative numerical simulation. In the

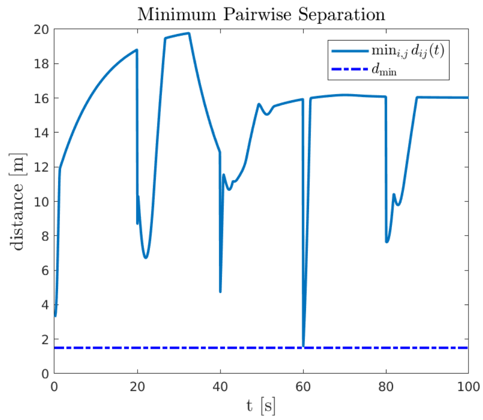

Fig. 3. Minimum pairwise separation.

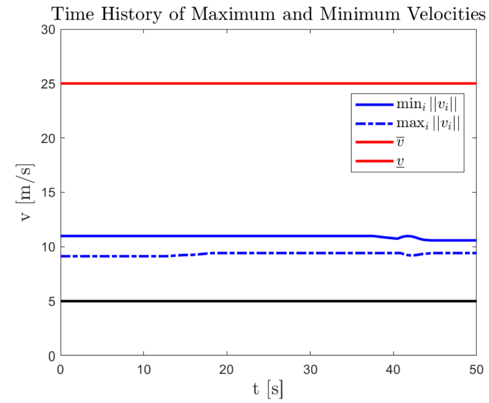

Fig. 4. Time history of minimum velocity and maximum velocity.

simulation, the potential function we choose is:

$$\psi(x) = \begin{cases} \log(\cosh(x - \hat{d})) & \text{if } x < \hat{d} \\ 0 & \text{otherwise} \end{cases} \tag{52}$$

the gradient of ψ is given by:

$$\phi(x) = \begin{cases} \tanh(x - \hat{d}) & \text{if } x < \hat{d} \\ 0 & \text{otherwise} \end{cases} \tag{53}$$

We let $\psi_b = \psi$ and $\phi_b = \phi$. Let Ω be the polyhedron whose walls are defined by:

$$A = \begin{bmatrix} 1 & 0 & 0 \\ -1 & 0 & 0 \\ 0 & 1 & 0 \\ 0 & -1 & 0 \\ 0 & 0 & 1 \\ 0 & 0 & -1 \end{bmatrix}, \quad b = \begin{bmatrix} 1000 \\ 0 \\ 40 \\ -40 \\ 40 \\ -40 \end{bmatrix}. \tag{54}$$

Other parameters for numerical simulation are given in Table I. Based on the parameters, we can achieve the feasible $c^* = 8.3069$. The configurations of sUAS's for every 20 seconds after a new group of sUAS are presented in Figure 2.

In this experiment, the set $\mathcal{A} \triangleq \{(x, y, z)| - 20 \leq y \leq 20, -20 \leq z \leq 20, 0 \leq x \leq 1000\}$, and it be observed that the configuration converges. We also plot the minimum pairwise separation between sUAS's in the traffic link in Figure 3. It can can be observed that all the sUAS's satisfy the minimum separation rule at all time. Similarly, it can be seen in Figure 4 that the minimum and maximum velocity constraints are always satisfied. This simulation shows that with our designed control protocol and entry condition, sUAS's are able to enter a single link safely and regulate their speeds and separations. The fundamental benefit of our control protocol based sUAS traffic management is not limited to achieve a collective behavior, but increase the amount of traffic a single link can take in a short period of time. Under our simulation, at least 2 sUAS can enter the link at every 20 seconds, which allows 360 sUAS's to travel across this link per hour. Such a great amount of traffic is formidable in the classical trajectory file/review process for traffic management if all the operators file their trajectory individually. The trajectory reviewing for this amount of traffic can also be overburden for the UTM.

V. Conclusion

In this article, we have proposed a new control protocol design and analysis method which can safely manage a large number of sUAS's, thereby improving scalability of the UTM. By taking the benefits of the autonomous nature of the sUAS's, we reformulated the traffic management problem as a distributed coordination control for multi-agent systems. We formally defined the sUAS's behaviors regularization problem in a single traffic link and proposed a control protocol to achieve the control objectives without violating the operation constraints. Further, we have analyzed the proposed control protocol and developed the condition for sUAS's entering a traffic link. This entry condition can be successfully converted to traffic management criteria/rules. In the numerical experiments, the proposed control protocol has been shown to be effective, and the entry condition is validated. This work offers a fundamental framework and theoretical results for studying a micro-scope traffic regularization problem in more complex traffic network elements, such as merge links and split links.

References

[1] A. S. Aweiss, B. D. Owens, J. Rios, J. R. Homola, and C. P. Mohlenbrink, "Unmanned aircraft systems (UAS) traffic management (UTM) national campaign II," in *Proc. AIAA Inf. Syst.-AIAA Infotech Aerosp.*, Jan. 2018, p. 1727.

[2] *Summary of Small Unmanned Aircraft Rule (Part 107)*, Federal Aviation Admin., Washington, DC, USA, 2016.

[3] M. Johnson *et al.*, "Flight test evaluation of an unmanned aircraft system traffic management (UTM) concept for multiple beyond-visual-line-of-sight operations," Nat. Aeronaut. Space Admin., Washington, DC, USA, Tech. Rep. 20170011344, 2017.

[4] *UTM: Air Traffic Management for Low-Altitude Drones*, Nat. Aeronaut. Space Admin., Washington, DC, USA, 2015.

[5] *NASA Conducts 'Out of Sight' Drone Tests in Nevada*, Nat. Aeronaut. Space Admin., Washington, DC, USA, 2015.

[6] T. Jiang, J. Geller, D. Ni, and J. Collura, "Unmanned aircraft system traffic management: Concept of operation and system architecture," *Int. J. Transp. Sci. Technol.*, vol. 5, no. 3, pp. 123–135, Oct. 2016.

[7] L. Ren *et al.*, "Small unmanned aircraft system (sUAS) trajectory modeling in support of UAS traffic management (UTM)," in *Proc. 17th AIAA Aviation Technol., Integr., Oper. Conf.*, Jun. 2017, p. 4268.

[8] C. A. Ippolito, K. S. Krishnakumar, V. Stepanyan, A. Bencomo, A. Chakrabarty, and S. Hening, "An autonomy architecture concept for high-density operations of small UAS in urban environments," in *Proc. AIAA Scitech Forum*, San Diego, CA, USA, Jan. 2019, doi: 10.2514/6.2019-0689.

[9] B. Weib, M. Naderhirn, and L. Re, "Global real-time path planning for UAVs in uncertain environment," in *Proc. IEEE Int. Conf. Control Appl., IEEE Int. Symp. Intell. Control*, Oct. 2006, pp. 2725–2730.

[10] N. Aeronautics and S. Administration, "Unmanned aircraft system (UAS) traffic management (UTM): Enabling civilian low-altitude airspace and unmanned aerial system operations," Federal Aviation Admin., Washington, DC, USA, Tech. Rep., 2020.

[11] I. Lopez and C. R. Mclnnes, "Autonomous rendezvous using artificial potential function guidance," *J. Guid., Control, Dyn.*, vol. 18, no. 2, pp. 237–241, Mar. 1995.

[12] J. Ruchti, R. Senkbeil, J. Carroll, J. Dickinson, J. Holt, and S. Biaz, "Unmanned aerial system collision avoidance using artificial potential fields," *J. Aerosp. Inf. Syst.*, vol. 11, no. 3, pp. 140–144, Mar. 2014.

[13] M. Arcak, "Passivity as a design tool for group coordination," *IEEE Trans. Autom. Control*, vol. 52, no. 8, pp. 1380–1390, Aug. 2007.

[14] C. W. Reynolds, "Flocks, herds and schools: A distributed behavioral model," in *Proc. 14th Annu. Conf. Comput. Graph. Interact. Techn. (SIGGRAPH)*, 1987, pp. 25–34.

[15] R. Olfati-Saber, "Flocking for multi-agent dynamic systems: Algorithms and theory," *IEEE Trans. Autom. Control*, vol. 51, no. 3, pp. 401–420, Mar. 2006.

[16] H. G. Tanner, A. Jadbabaie, and G. J. Pappas, "Flocking in fixed and switching networks," *IEEE Trans. Autom. Control*, vol. 52, no. 5, pp. 863–868, May 2007.

[17] B. Lei, W. Li, and F. Zhang, "Flocking algorithm for multi-robots formation control with a target steering agent," in *Proc. IEEE Int. Conf. Syst., Man Cybern.*, Oct. 2008, pp. 3536–3541.

[18] Q. Li and Z.-P. Jiang, "Flocking control of multi-agent systems with application to nonholonomic multi-robots," *Kybernetika*, vol. 45, no. 1, pp. 84–100, 2009.

[19] J. A. Gouvea, F. Lizarralde, and L. Hsu, "Potential function formation control of nonholonomic mobile robots with curvature constraints," *IFAC Proc. Volumes*, vol. 44, no. 1, pp. 11931–11936, Jan. 2011.

[20] J. Jin, Y.-G. Kim, S.-G. Wee, and N. Gans, "Consensus based attractive vector approach for formation control of nonholonomic mobile robots," in *Proc. IEEE Int. Conf. Adv. Intell. Mechatronics (AIM)*, Jul. 2015, pp. 977–983.

[21] S. Mastellone, D. M. Stipanović, C. R. Graunke, K. A. Intlekofer, and M. W. Spong, "Formation control and collision avoidance for multi-agent non-holonomic systems: Theory and experiments," *Int. J. Robot. Res.*, vol. 27, no. 1, pp. 107–126, Jan. 2008.

[22] D. Sun, C. Kwon, and I. Hwang, "Hybrid flocking control algorithm for fixed-wing aircraft," *J. Guid., Control, Dyn.*, vol. 42, no. 11, pp. 2443–2455, Nov. 2019.

[23] Q. Li, J. Yuan, B. Zhang, and H. Wang, "Artificial potential field based robust adaptive control for spacecraft rendezvous and docking under motion constraint," *ISA Trans.*, vol. 95, pp. 173–184, Dec. 2019.

[24] W. Yu and G. Chen, "Robust adaptive flocking control of nonlinear multi-agent systems," in *Proc. IEEE Int. Symp. Comput.-Aided Control Syst. Design*, Sep. 2010, pp. 363–367.

[25] Y. Kuriki and T. Namerikawa, "Consensus-based cooperative formation control with collision avoidance for a multi-UAV system," in *Proc. Amer. Control Conf.*, Jun. 2014, pp. 2077–2082.

[26] *Unmanned Aircraft System (UAS) Traffic Management (UTM) Concept of Operations V2.0*, Office of NextGen, New Delhi, India, 2020.

[27] T. Van Woensel and N. Vandaele, "Modeling traffic flows with queueing models: A review," *Asia-Pacific J. Oper. Res.*, vol. 24, no. 4, pp. 435–461, Aug. 2007.

[28] H. K. Khalil and J. W. Grizzle, *Nonlinear Systems*, vol. 3. Upper Saddle River, NJ, USA: Prentice-Hall, 2002.

[29] K. Tanaka, "Homoclinic orbits in a first order superquadratic Hamiltonian system: Convergence of subharmonic orbits," *J. Differ. Equ.*, vol. 94, no. 2, pp. 315–339, Dec. 1991.

[30] V. V. Kozlov and D. Treshchev, "Weak convergence of solutions of the Liouville equation for nonlinear Hamiltonian systems," *Theor. Math. Phys.*, vol. 134, no. 3, pp. 339–350, 2003.

[31] C. G. Broyden, "A new method of solving nonlinear simultaneous equations," *Comput. J.*, vol. 12, no. 1, pp. 94–99, Feb. 1969.

[32] U. Helmke and J. B. Moore, *Optimization and Dynamical Systems*. Berlin, Germany: Springer, 2012.

[33] F. Alvarez, "On the minimizing property of a second order dissipative system in Hilbert spaces," *SIAM J. Control Optim.*, vol. 38, no. 4, pp. 1102–1119, Jan. 2000.

[34] G. G. Rigatos, "Nonlinear Kalman filters and particle filters for integrated navigation of unmanned aerial vehicles," *Robot. Auto. Syst.*, vol. 60, no. 7, pp. 978–995, Jul. 2012.

[35] M. Bibuli, G. Bruzzone, M. Caccia, and L. Lapierre, "Path-following algorithms and experiments for an unmanned surface vehicle," *J. Field Robot.*, vol. 26, no. 8, pp. 669–688, Aug. 2009.

[36] X. Yu and Y. Zhang, "Sense and avoid technologies with applications to unmanned aircraft systems: Review and prospects," *Prog. Aerosp. Sci.*, vol. 74, pp. 152–166, Apr. 2015.

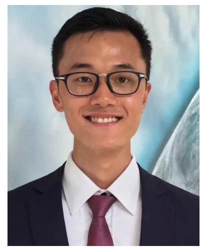

Jiazhen Zhou received the bachelor's degree in mechanical engineering from the University of Missouri and the master's degree in aeronautics and astronautics engineering from Purdue University, where he is currently pursuing the Ph.D. degree with the School of Aeronautics and Astronautics. His research interest includes control and optimization of transportation systems.

Dawei Sun received the bachelor's and master's degrees in aeronautics and astronautics engineering from Purdue University, where he is currently pursuing the Ph.D. degree with the School of Aeronautics and Astronautics. His research interests include hybrid system theory, resilient control, and distributed algorithms.

Inseok Hwang (Member, IEEE) received the Ph.D. degree in aeronautics and astronautics from Stanford University, Stanford, CA, USA, in 2004. He is currently a Professor with the School of Aeronautics and Astronautics, Purdue University, West Lafayette, IN, USA. His research interests include modeling, estimation, and control of cyber-physical systems and their applications to safety critical systems, such as aircraft/spacecraft/unmanned aerial systems, air traffic management, and multiagent systems. For his research, he leads the Flight Dynamics and Control/Hybrid Systems Laboratory, Purdue University. He is also an Associate Fellow of AIAA, and a member of the IEEE Control Systems Society and the IEEE Aerospace and Electronic Systems Society. He was a recipient of the NSF CAREER Award in 2008, was selected as one of the nation's brightest young engineers by the National Academy of Engineering (NAE) in 2008, and received the AIAA Special Service Citation in 2010. He is also an Associate Editor of the IEEE TRANSACTIONS ON AEROSPACE AND ELECTRONIC SYSTEMS and the *Asian Journal of Control*, and the Conference Editorial Board Member of the IEEE Control Systems Society.

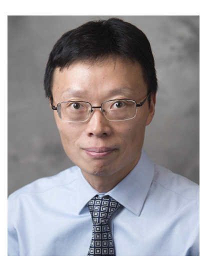

Dengfeng Sun (Senior Member, IEEE) received the bachelor's degree in precision instruments and mechanology from Tsinghua University, China, the master's degree in industrial and systems engineering from Ohio State University, and the Ph.D. degree in civil engineering from the University of California at Berkeley. He is currently an Associate Professor with the School of Aeronautics and Astronautics, Purdue University, West Lafayette, IN, USA. His research interests include control and optimization of large scale systems and their applications in aerospace engineering.